 doi:10.20944/preprints202208.0152.v1

Article

The N-terminal part of the 1A domain of desmin is a hot spot region for putative pathogenic *DES* mutations affecting the filament assembly

Andreas Brodehl [1,*], Stephanie Holler [1], Jan Gummert [1] and Hendrik Milting [1,*]

[1] Erich and Hanna Klessmann Institute, Heart and Diabetes Center NRW, University Hospital of the Ruhr-University Bochum, Georgstrasse 11, 32545 Bad Oeynhausen, Germany. abrodehl@hdz-nrw.de, sholler@hdz-nrw.de (S.H.); jgummert@hdz-nrw.de (J.G.) and hmilting@hdz-nrw.de.

* Correspondence: abrodehl@hdz-nrw.de; Tel. +49-5731-973530 (A.B.) or hmilting@hdz-nrw.de; Tel. +49-5731-973510 (H.M.).

Abstract: Desmin is the major intermediate filament protein of all three muscle cell types and connects different cell organelles and multi-protein complexes like the cardiac desmosomes. Several pathogenic mutations in the *DES* gene cause different skeletal and cardiac myopathies. However, the significance of the majority of *DES* missense variants is currently unknown since functional data are lacking. To determine whether desmin missense mutations within the highly conserved 1A coil domain cause a filament assembly defect, we generated a set of variants with unknown significance and analyzed systematically the filament assembly in transfected SW13 and H9c2 cells using confocal microscopy. We found that mutations in the N-terminal part of the 1A coil domain affect the filament assembly leading to the cytoplasmic desmin aggregation. In contrast, mutant desmin in the C-terminal part of the 1A coil domain form filamentous structures comparable to wild-type desmin. Our findings suggest that the N-terminal part of the 1A coil domain is a hot spot for pathogenic desmin mutations, which affect the desmin filament assembly leading in consequence to skeletal and/or cardiac myopathies. This study may have relevance for the genetic counselling of patients carrying variants in the 1A coil domain of the *DES* gene.

Keywords: Desmin; Myopathy; Cardiomyopathy; Intermediate Filaments; Cytoskeleton; Myofibrillar Myopathy (MFM); Desminopathy; Desmosomes; Protein Aggregation.

1. Introduction

Desminopathies become manifest clinically as different cardiomyopathies and/or skeletal myopathies [1,2]. The clinical spectrum of desminopathies is wide and heterogenous and includes different skeletal myopathies and cardiomyopathies like dilated (DCM) [3-5], arrhythmogenic (ACM) [6,7], hypertrophic (HCM) [8,9], restrictive (RCM) [10,11] or non-compaction cardiomyopathy (NCCM) [12,13]. Several patients develop a combined cardiac and a skeletal muscle phenotype and even within the same family different phenotypes can be present [14].

Genetically, desminopathies are caused by *DES* mutations [15,16]. The human *DES* gene (MIM, *125660) consist of nine exons localized on chromosome 2 [17] and encodes the major muscle-specific intermediate filament (IF) protein desmin. The majority of known pathogenic *DES* mutations are heterozygous missense or small in-frame deletion mutations. Of note, nonsense or frameshift mutations in the *DES* gene are rare and cause in most cases only as homozygous or compound heterozygous mutations a phenotype [18,19].

Desmin connects different cell organelles and multi-protein complexes [20] like the Z-bands [21], costameres [22] and desmosomes [23]. Therefore, the desmin filaments have high relevance for the structural integrity of (cardio)myocytes [24]. Mutant desmin

Preprints (www.preprints.org) | NOT PEER-REVIEWED | Posted: 8 August 2022 doi:10.20944/preprints202208.0152.v1

disorganizes the complex cytoskeleton network and disrupts the sarcomeric organization [25].

Desmin consists of three different domains, the N-terminal head, a central rod and a C-terminal tail domain [1]. The central α-helical rod domain consists of two coil subdomains 'coil-1' and 'coil-2' separated by a non-helical linker L12 [26]. Coil-1 contains a second non-helical linker L1 dividing coil-1 into a smaller 1A and a larger 1B region [26,27]. A coiled-coil dimer is formed by dimerization of the central rod domains [28,29]. These dimers form antiparallel tetramers [27]. The antiparallel tetramers laterally anneal into unit length filaments (ULFs), which are the essential building blocks of the desmin filaments [30]. In addition, IFs can fuse end to end and subunits are intercalary exchanged [31,32]. Pathogenic desmin mutations disturb the complex filament assembly at different steps [33,34] and have a dominant effect on the wild-type form [3]. This explains on the molecular level the dominant inheritance of most *DES* missense mutations.

Currently, it is difficult to predict and classify novel *DES* missense variants in human genetics since functional data are missing in most cases. Therefore, most of them must be classified as variants of unknown significance (VUS) according to the guidelines of the American College of Medical Genetics and Genomics (ACMG) [35]. Especially, because only a few pathogenic *DES* mutations -some with a severe clinical phenotype- have been described in the 1A subdomain [3,6,13,36-39], we addressed the question which of the known VUS within the *DES* 1A coil domain affect the desmin filament assembly.

To answer this question, we inserted all known VUS in the 1A subdomain listed in the ClinVar database (https://www.ncbi.nlm.nih.gov/clinvar/, assessed 21th July 2022) [40] and the Human Gene Mutation Database (https://www.hgmd.cf.ac.uk/, assessed 21th July 2022) [41] into expression plasmids and performed cell transfection experiments using SW13 and H9c2 cells in combination with cytochemistry and confocal microscopy. We found that the N-terminal part of the 1A desmin subdomain is a hot spot for variants affecting the filament assembly *in vitro*. Our functional data may contribute to an improved understanding of novel *DES* mutations within this subdomain which may support variant classification and genetic counselling of affected patients in the future.

2. Materials and Methods

2.1. Plasmid generation and site-directed mutagenesis

The cloning of the plasmid pEYFP-N1-DES-WT has been previously described [34]. All mutations were inserted into this plasmid by site-directed mutagenesis (SDM) using the QuikChange Lightning kit according to the manufacturer's instruction (Agilent Technologies, Santa Clara, CA, USA). The used primers (synthezied by Mycrosynth, Balgach, Switzerland) are listed in Table A1 (see Appendix A). The *DES* encoding regions in all plasmids were verifed by Sanger sequencing (Macrogen, Amsterdam, Netherland) using the CMV_for and the EGFP_rev primer (Table A1, Appendix A). Sequencing data were analyzed using SnapGene software Version 6.1 (GSL Biotech LLC, San Diego, CA, USA). The plasmids were prepared using the Plasmid Miniprep Kit (Thermo Fisher Scientific, Waltham, MA, USA). All plasmids are available from the corresponding author (A.B.).

2.2. Cell culture

SW-13 and H9c2 (ATCC, Manassas, VA, USA) were cultured in Dulbecco's Modified Eagle Medium (DMEM, Thermo Fisher Scientific) supplemented with 10 % fetal calf serum and penicilline/streptomycine at 37 °C and 5 % CO_2. SW-13 cells do not express desmin or any other cytoplasmic IF protein [42], whereas H9c2 cells are cardiac myoblasts with an endogenous desmin expression [43]. Cells were splitted every three days using trypsin/ethylenediaminetetraacetic acid (Thermo Fisher Scientific).

 doi:10.20944/preprints202208.0152.v1

2.3. Cell transfection

The cells were splitted one day before transfection and were cultured in 8 well µ-Slide chambers (ibidi, Gräfelfing, Germany). Lipofectamin 3000 (Thermo Fisher Scientific) was used according to the manufacturer's instruction for cell transfection. 250 ng of the plasmid were used per well and the ratio of Lipofectamin 3000 to plasmid was 3:1.

2.4. Cell fixation and immuncytochemistry

24 h after cell transfection, the cells were gently washed with phosphate buffered saline (PBS, Thermo Fisher Scientific). Afterwards the cells were fixed with 4 % HistoFix (Carl Roth, Karlsruhe, Germany) for 15 min at room temperature (RT). Then the cells were washed twice with PBS and permeabilized using 0.1 % Triton X-100 (solved in PBS) for 15 min at RT. After washing with PBS the cells were incubated for 40 min at RT with phalloidin conjugated with Texas-Red (1:400, Thermo Fisher Scientific) to stain the F-actin. 4',6-diamidino-2-phenylindole (DAPI, 1 µg/mL) was used for staining of the nuclei for 5 min at RT. After final washing steps, the cells were stored in PBS in the µ-Slide chambers until microscopy at 4 °C in the dark.

2.5 Confocal laser scanning microscopy

The TCS SP8 confocal system (Leica Microsystems, Wetzlar, Germany) was used in combination with the Application Suite X software (Leica Microsystems) for confocal fluorescence microscopy of the transfectected cells. DAPI was excited at 405 nm and the emission was detected in the range between 410- 460 nm. Enhanced yellow fluorescent protein (EYFP) was excited at 488 nm and the emission was detected in the range between 493-560 nm. Texas-Red was exited at 552 nm and the emission was detected in the range between 570-781 nm. The excitation and emission detection of the three fluorescence channels were sequentially performed.

2.6 Molecular visualization

The desmin dimer structure was predicted using AlphaFold-Multimer [44] and was visualized using the PyMOL Molecular Graphics System Version 2.5.2 (Schrödinger, New York, NY, USA).

2.7 Statistical analysis

Over hundred cells were manually analyzed per transfection experiments and three independent transfection experiments were analyzed per construct and cell line (n=3). One-way ANOVA followed by Bonferroni's multiple comparisons test was performed using GraphPad Prism Version 9.0 (GraphPad Software, San Diego, CA, USA). The presented data are given as mean ± standard deviation (SD).

3. Results

Most variants within the desmin 1A subdomain are currently classified as VUS. This subdomain is highly conserved in different type-3 intermediate filament proteins as well as between different species (Figure 1A-B). However, the impact of specific variants is unknown in most cases. To evaluate the impact of 34 different VUS within the desmin 1A subdomain listed in the ClinVar database (Figure 1C), we inserted them via SDM into expression plasmids and performed cell culture transfection experiments in combination with confocal microscopy. We used SW-13 cells, because this cell line expresses no endogenous desmin or any other cytoplasmic intermediate filament proteins. Additionally, we used the cardiac myoblast cell line H9c2 for these experiments because

Preprints (www.preprints.org) | NOT PEER-REVIEWED | Posted: 8 August 2022 doi:10.20944/preprints202208.0152.v1

this cell line expresses endogenous desmin. The wild-type desmin forms in both cell lines filamentous structures (Figure 1D-E).

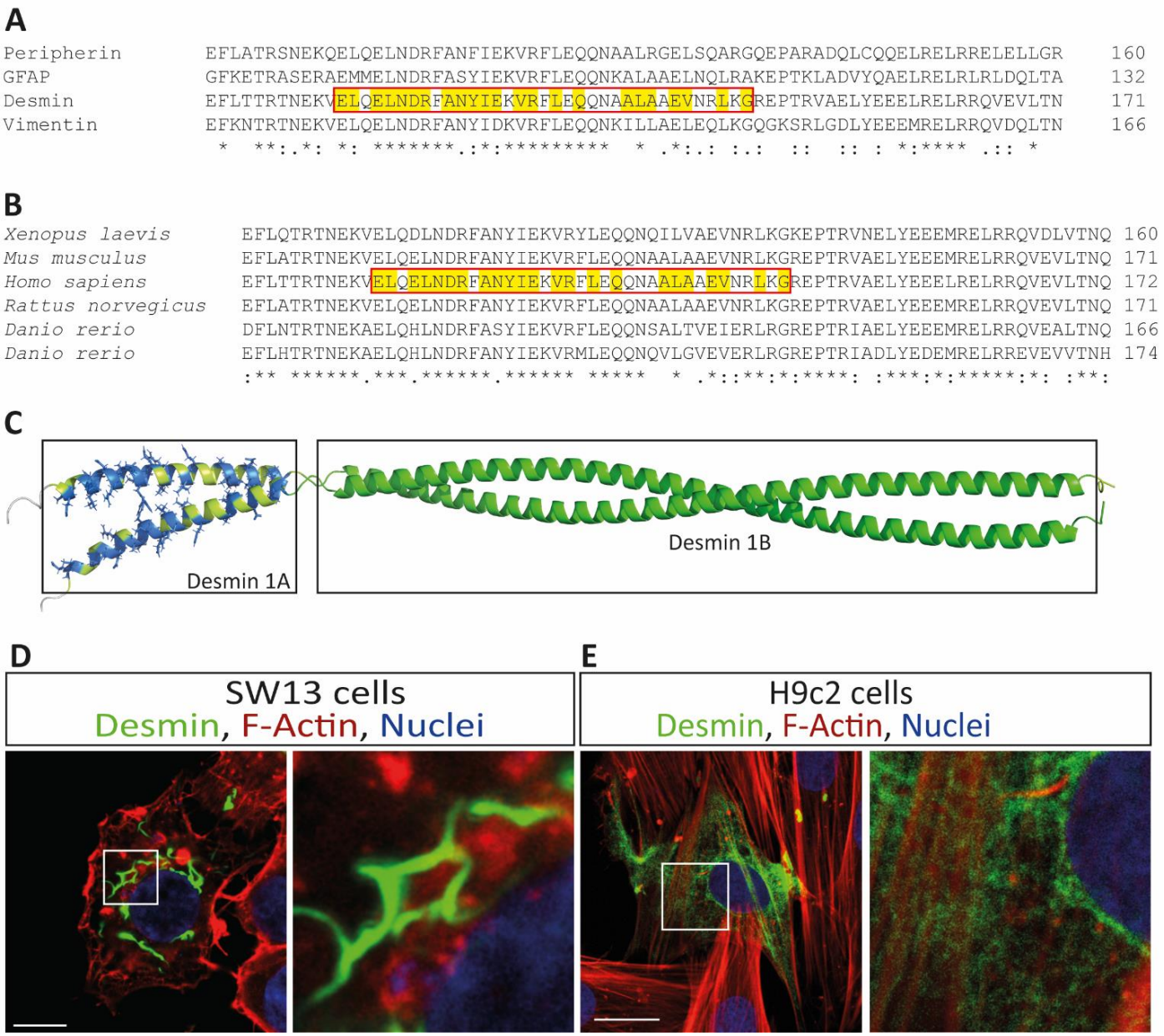

Figure 1. (A) Partial sequence alignment of different human type-3 intermediate filament proteins. The highly conserved 1A domain is shown by a red box and the positions of variants with unknown significance are highlighted in yellow. **(B)** Partial sequence alignment of desmin of different species. The highly conserved 1A domain is shown by a red box and the positions of variants with unknown significance are highlighted in yellow. **(C)** Structural overview about the desmin coil 1A and coil 2 subdomains. The positions of variants with unknown significance are highlighted in blue. Representative cell images of desmin-wild-type transfected SW13 **(D)** and H9c2 cells **(E)** are shown. Desmin is shown in green, F-actin in red and the nuclei in blue. Scale bars represent 10 μm **(D)** or 20 μm **(E)**.

In contrast to the wild-type desmin, the mutant forms p.E111G, p.L112R, p.L115P, p.N116I, p.N116K, p.R118C and p.R118S localized at the N-terminus of the 1A subdomain, disturb the cellular filament formation *in vitro* and cause a cytoplasmic desmin aggregation in both cell lines (Figure 2). The desmin mutants p.E114G and p.D117H form filamentous networks comparable to the wild-type form (Figures 2C and 2G).

Preprints (www.preprints.org) | NOT PEER-REVIEWED | Posted: 8 August 2022 doi:10.20944/preprints202208.0152.v1

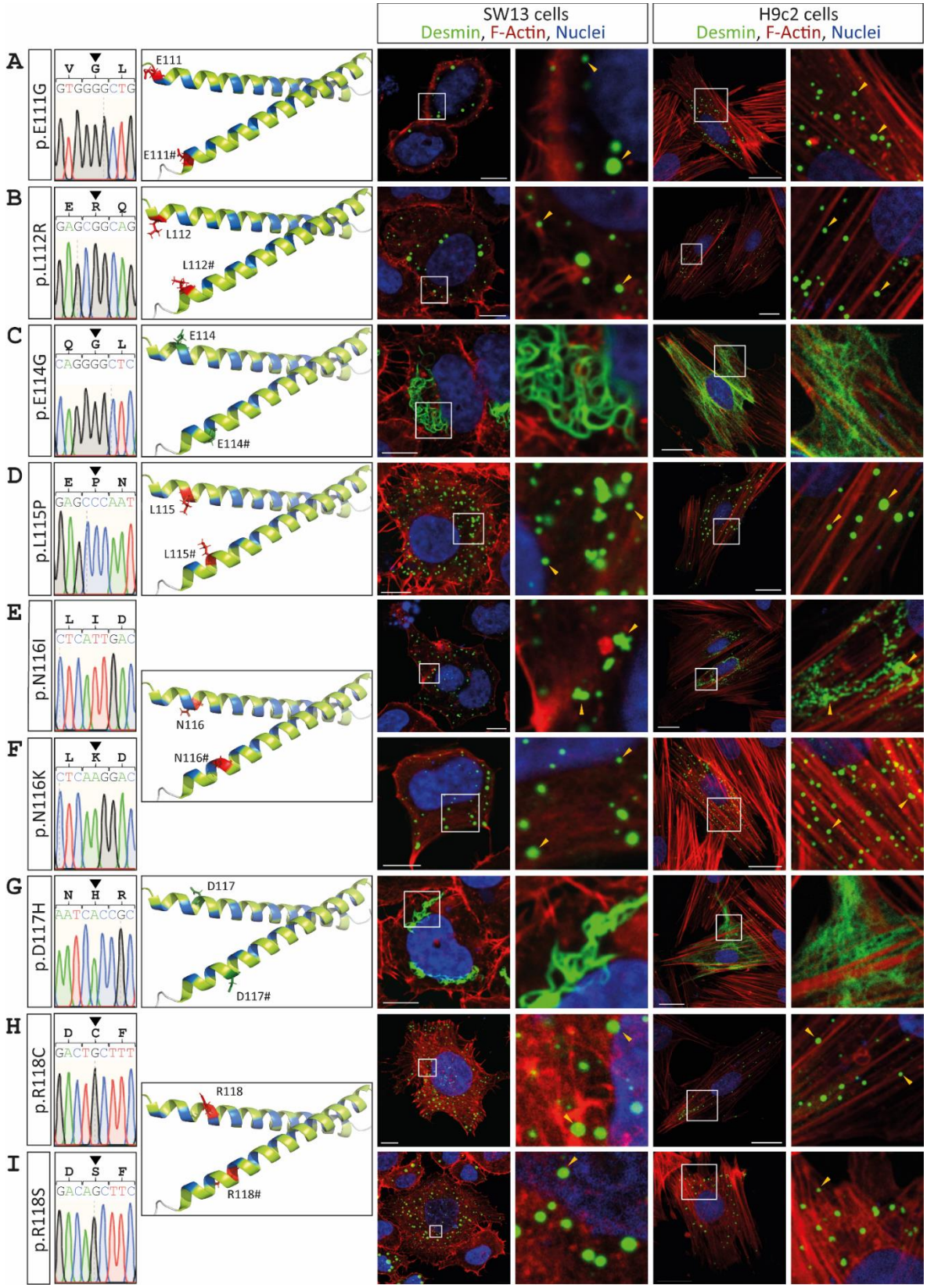

Figure 2. Overview about the *DES* variants **(A)** p.E111G, **(B)** p.L112R, **(C)** p.E114G, **(D)** p.L115P, **(E)** p.N116I, **(F)** p.N116K, **(G)** p.D117H, **(H)** p.R118C and **(I)** p.R118S. Sections of Sanger sequencing electropherograms are shown. The affected amino acids are shown in the molecular overview as sticks in red or green depending on aggregate or filament formation. Representative cell images are shown. Desmin is shown in green, F-actin in red and the nuclei in blue. Of note, the mutants p.E111G, p.L112R, p.L115P, p.N116I, p.N116K, p.R118C and p.R118S are forming abnormal cytoplasmic desmin aggregates (yellow arrow heads). Scale bars represent 10 µm (SW13 cells) or 20 µm (H9c2 cells).

Preprints (www.preprints.org) | NOT PEER-REVIEWED | Posted: 8 August 2022 doi:10.20944/preprints202208.0152.v1

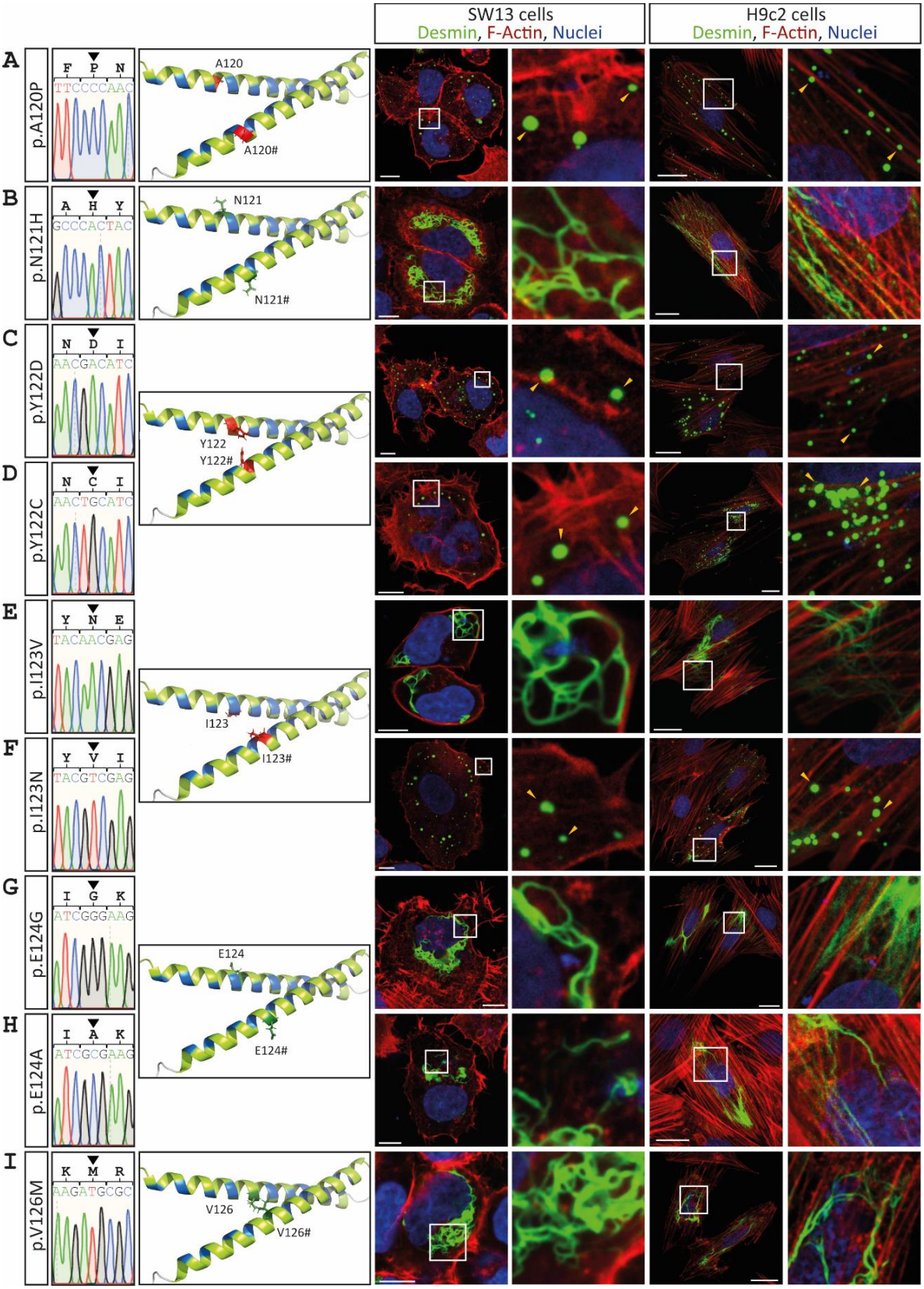

Figure 3. Overview on the *DES* variants **(A)** p.A120P, **(B)** p.N121H, **(C)** p.Y122D, **(D)** p.Y122C, **(E)** p.I123V, **(F)** p.I123N, **(G)** p.E124G, **(H)** p.E124A and **(I)** p.V126M. Sections of Sanger sequencing electropherograms are shown. The affected amino acids are shown in the molecular overview as sticks in red or green depending on its aggregate or filament formation activity. Representative cell images are shown. Desmin is given in green, F-actin in red and nuclei in blue. Of note, the mutants p.A120P, p.Y122D, p.Y122C and p.I123N are forming abnormal cytoplasmic desmin aggregates (yellow arrow heads). Scale bars represent 10 µm (SW13 cells) or 20 µm (H9c2 cells).

Preprints (www.preprints.org) | NOT PEER-REVIEWED | Posted: 8 August 2022 doi:10.20944/preprints202208.0152.v1

The desmin mutants p.A120P, p.Y122D, p.Y122C, p.I123N, p.V126L, p.R127G and p.R127P, which are likewise localized in the N-terminal part of the 1A subdomain, cause comparable cytoplasmic desmin aggregates of different sizes (Figures 3 and 4). However, some VUS localized in the N-terminal part of the highly conserved 1A subdomain (p.D117H, p.N121H, p.I123V, p.E124G/A and p.V126M) form regular intermediate filaments comparable to the wild-type desmin (Figure 3). Similarly, all VUS localized in the C-terminal part of the 1A subdomain (p.L129R, p.Q131K, p.A135V, p.L136V, p.L136H, p.A137D, p.E139Q, p.E139K, p.V140M, p.V140L, p.L143V, p.L143P and p.G145D) do not interfere with filament formation (Figure 4-5). Even severe amino acid exchanges of a negative to a positive amino acid (p.E139K) do not affect filament formation (Figure 5B). Comparably, the insertion of a proline at position 143 (p.L143P) does not affect desmin filament formation (Figure 5F). Quantification of >100 transfected cells in three independent transfection experiments verified these filament formation defects (Figure 6A). Of note, all missense variants leading to a filament assembly defect are localized within the N-terminal part of the 1A desmin subdomain, whereas the C-terminal mutants do not affect the filament formation (Figure 6B-D).

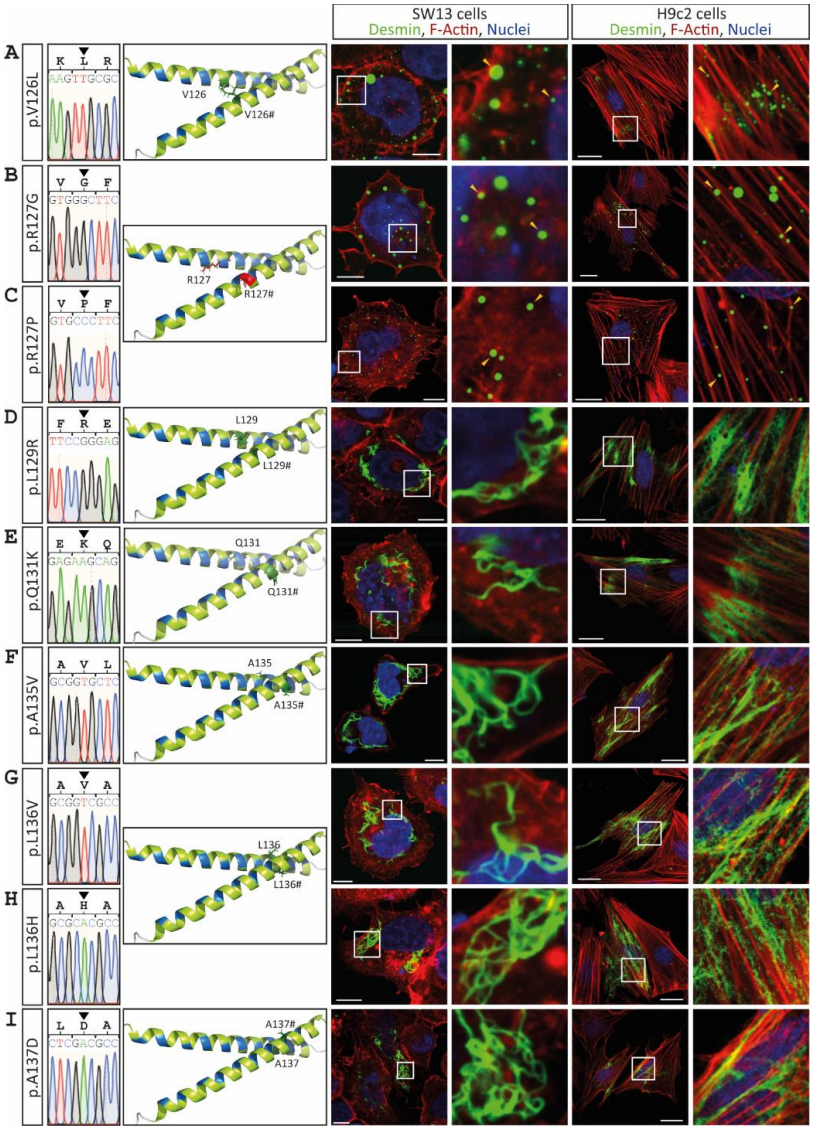

Figure 4. Overview about the *DES* variants **(A)** p.V126L, **(B)** p.R127G, **(C)** p.R127P, **(D)** p.L129R, **(E)** p.Q131K, **(F)** p.A135V, **(G)** p.L136V, **(H)** p.L136H and **(I)** p.A137D. Sections of Sanger sequencing electropherograms are shown. The affected amino acids are shown in the molecular overview as sticks in red or green depending on aggregate or filament formation. Representative cell images are shown. Desmin is shown in green, F-actin in red and the nuclei in blue. Of note, the mutants p.V126L, p.R127G and p.R127P form abnormal cytoplasmic desmin aggregates (yellow arrow heads). Scale bars represent 10 µm (SW13 cells) or 20 µm (H9c2 cells).

Preprints (www.preprints.org) | NOT PEER-REVIEWED | Posted: 8 August 2022 doi:10.20944/preprints202208.0152.v1

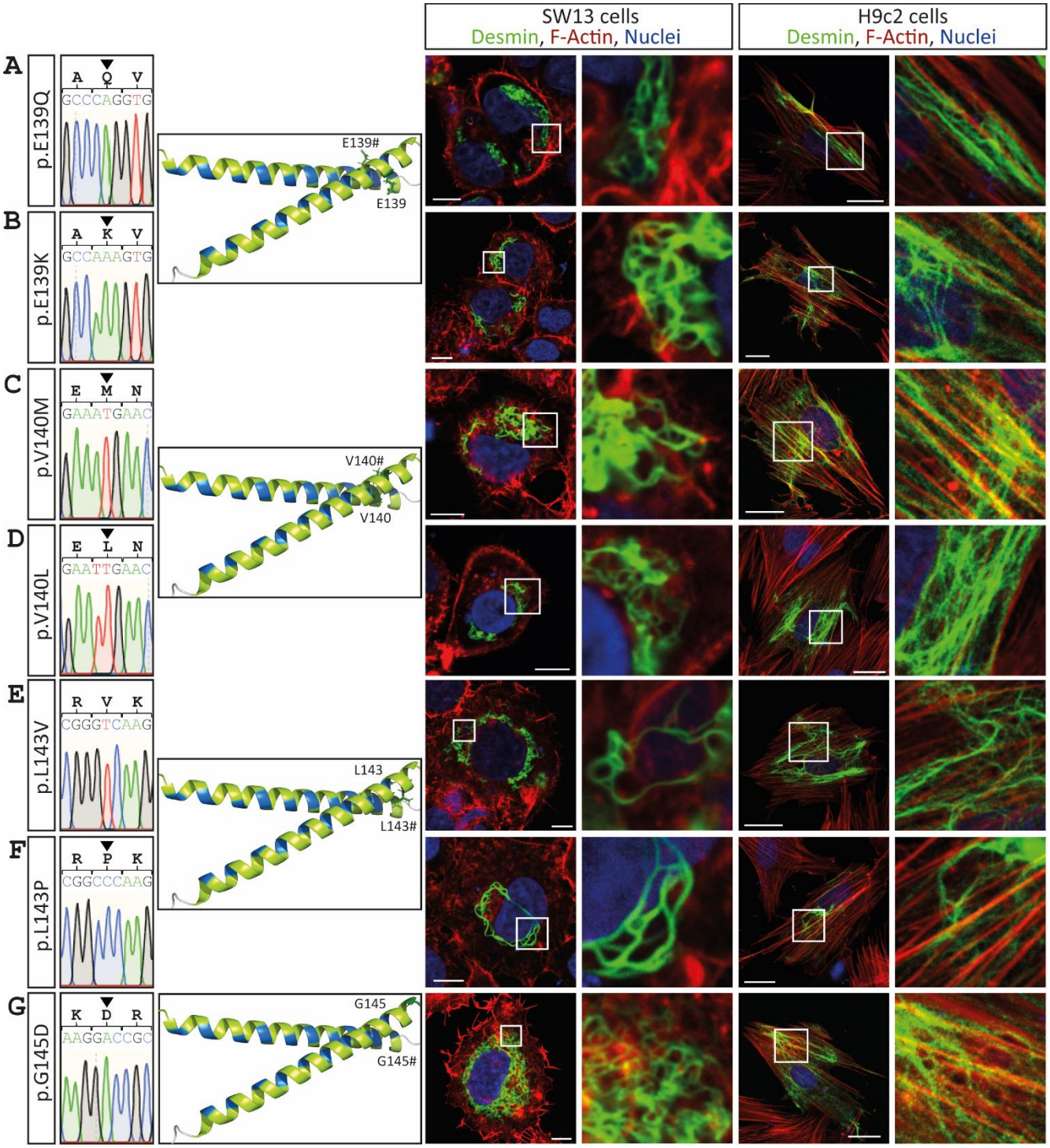

Figure 5. Overview on the *DES* variants **(A)** p.E139Q, **(B)** p.E139K, **(C)** p.V140M, **(D)** p.V140L, **(E)** p.L143V, **(F)** p.L143P and **(G)** p.G145D. Sections of Sanger sequencing electropherograms are shown. The affected amino acids are shown in the molecular overview as sticks in red or green depending on aggregate or filament formation. Representative cell images are shown. Desmin is shown in green, F-actin in red and nuclei in blue. None of these mutants forms abnormal cytoplasmic desmin aggregates. Scale bars represent 10 µm (SW13 cells) or 20 µm (H9c2 cells).

Preprints (www.preprints.org) | NOT PEER-REVIEWED | Posted: 8 August 2022 doi:10.20944/preprints202208.0152.v1

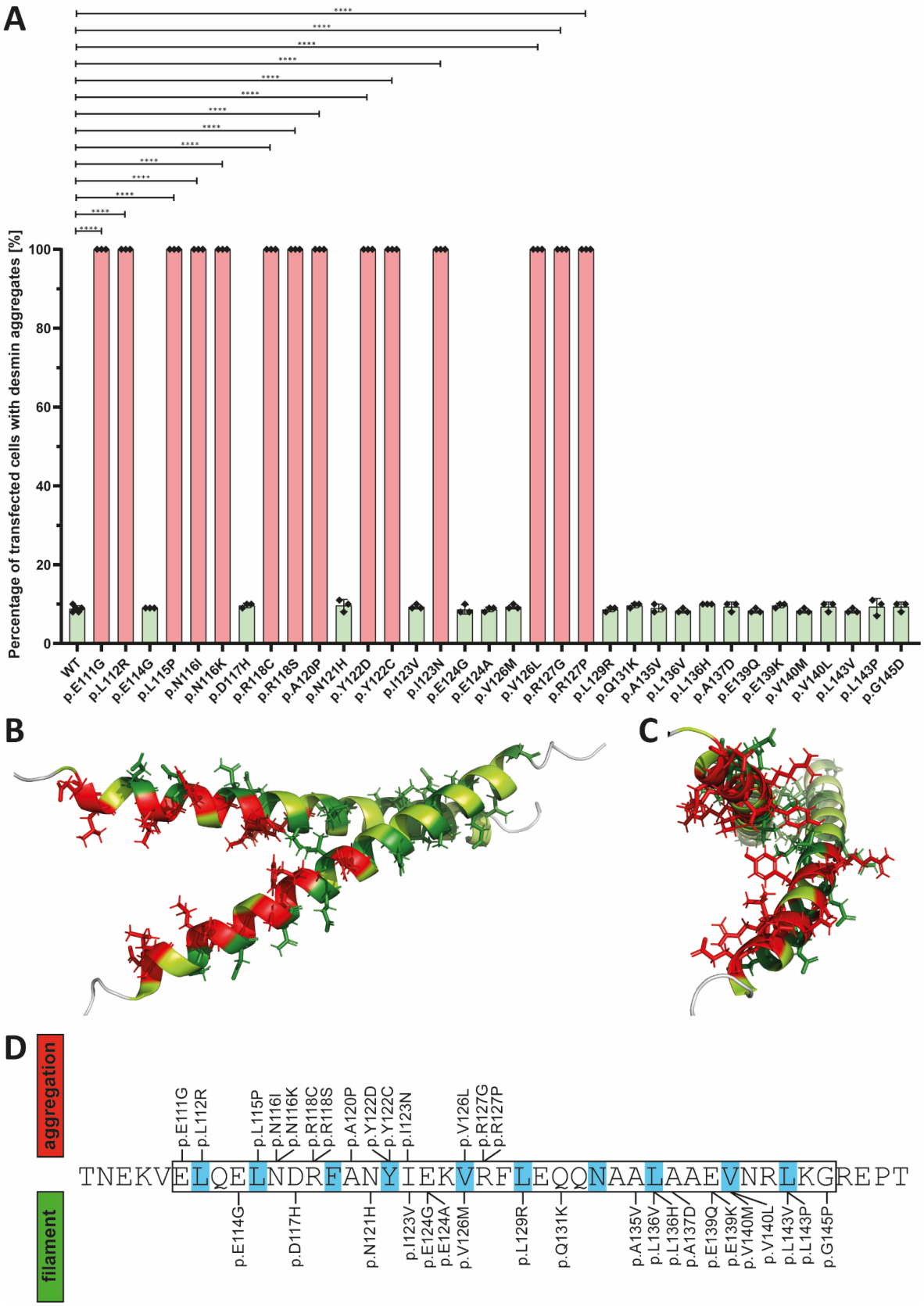

Figure 6. (A) Statistical analysis of aggregate formation in transfected SW-13 cells. One-way ANOVA followed by Bonferroni's multiple comparisons test was used for analysis. **** p-value < 0.0001. **(B-C)** Structural overview about the desmin 1A subdomain. The positions of the mutant amino acids leading to abnormal cytoplasmic desmin aggregation are shown in red and mutant amino acids without filament formation defects are given in green. **(D)** Schematic overview about the localization of the VUS localized in the desmin 1A domain. The heptad is highlighted in blue.

 doi:10.20944/preprints202208.0152.v1

4. Discussion

In this study, we found that several VUS localized in the N-terminal part of the desmin 1A subdomain affect the filament assembly *in vitro* leading to an abnormal cytoplasmic protein aggregation and can be classified in conclusion as likely pathogenic mutations. Our results indicate that this desmin region is a hot spot for pathogenic mutations leading to skeletal myopathies or cardiomyopathies.

Different criteria like *e.g.* co-segregation within the family or absence in healthy controls are frequently used in cardiovascular genetics for pathogenicity classification and risk assessment [35]. However, for most novel rare variants the pathogenetic impact is unknown and hardly to predict. As a database resource for genetic variants, the identified VUS are collected i.e. in the ClinVar database (ClinVar (nih.gov)) and/or the Human Gene Mutation Database (https://www.hgmd.cf.ac.uk). According to the ACMG guidelines, functional data is a strong criterion for pathogenicity (PS3) and can support the classification and pathogenetic evidence of specific VUS [35]. Some pathogenic or likely pathogenic variants in the desmin 1A subdomain have been recently characterized [6,36,38,39,45]. However, variants within the 1A desmin subdomain are less characterized compared to the desmin coil-2 or the tail domains [33,46,47]. Therefore, we focused in this study on VUS distributed over the complete 1A desmin subdomain. We inserted a set of 34 different variants classified in ClinVar as VUS into a desmin encoding expression plasmid and analyzed their cellular filament assembly by confocal microscopy. These experiments revealed for 14 different VUS (p.E111G, p.L112R, p.L115P, p.N116I, p.N116K, p.R118C, p.R118S, p.A120P, p.Y122D, p.Y122C, p.I123N, p.V126L, p.R127G and p.R127P) a severe filament assembly defect. These functional data support their classification as likely pathogenic variants (ACMG class 4) rather than VUS (ACMG class 3). However, we cannot exclude from our experiments that some of the other VUS change nanomolecular properties of the desmin filaments like previously described by Kreplak et al. i.e. for desmin-p.Q389P and p.D399Y [48].

Interestingly, the aggregate causing mutations cluster in the N-terminal part of the 1A desmin subdomain, whereas most of the C-terminal VUS do not affect the desmin filament formation in transfected SW-13 or H9c2 cells. These results indicate that the N-terminal part of the 1A subdomain is a putative hot spot region for pathogenic sequence variants in the desmin protein. In more detail, the amino acids leading to desmin aggregation are oriented into the inner part of the predicted desmin dimer model (Figure 6B-C), whereas mutations affecting amino acids oriented to the outer surface of the dimer like p.E114G, p.D117H or p.N121H have no impact on the *in vitro* filament assembly. It is known that this part of the 1A subdomain of the homologous IF protein vimentin is likewise involved in the tetramer formation [28]. However, the detailed molecular structure at the complete IF level is currently unknown. Interestingly, several pathogenic mutations in this part of the 1A subdomain of the homologous protein glial fibrillary acidic protein (GFAP) cause Alexander disease, which belongs to the leukodystrophies (MIM, #203450) [49-52]. Additionally, mutations in the N-terminal part of the 1A subdomain of lamin A/C (*LMNA*) cause congenital muscular dystrophy or Emery-Dreifuss muscular dystrophy (MIM, #181350) [53-55].

5. Conclusions

In conclusion, our study revealed a mutational hot spot region in the N-terminal part of the 1A desmin subdomain, where several missense mutations cause severe filament assembly defects. This suggests that novel *DES* missense mutations affecting this part of desmin should be considered as putative disease-causing variants and should be functionally analyzed.

Author Contributions: Conceptualization, A.B.; methodology, A.B.; validation, A.B.; formal analysis, A.B.; investigation, A.B. and S.H.; resources, J.G.; data curation, A.B.; writing—original draft preparation, A.B.; writing—review and editing, S.H, J.G. and H.M.; visualization, A.B.; supervision, A.B. and H.M.; project administration, A.B.; funding acquisition, A.B., J.G. and H.M. All authors have read and agreed to the published version of the manuscript.

 doi:10.20944/preprints202208.0152.v1

Funding: This research was funded by the Ruhr-University Bochum, grant number FoRUM, F937R2 (A.B. and H.M.). The APC was kindly funded by the DFG Open Access Publication Funds of the Ruhr-University Bochum. We are also greatful to the continuous support by the Erich and Hanna Klessmann-Foundation, Gütersloh, Germany.

Institutional Review Board Statement: Not applicable.

Informed Consent Statement: Not applicable.

Data Availability Statement: The published article includes the data generated or analyzed during this study. The used plasmids are available from the corresponding author (A.B.).

Conflicts of Interest: The authors declare no conflict of interest. The funders had no role in the design of the study; in the collection, analyses, or interpretation of data; in the writing of the manuscript; or in the decision to publish the results.

Appendix A

Table A1. Overview about the used oligonucleotids.

Name	Sequence (5′-3′)	Application
DES_E111G_for	CAACGAGAAGGTGGGGCTGCAGGAGCTCA	SDM
DES_E111G_rev	TGAGCTCCTGCAGCCCCACCTTCTCGTTG	SDM
DES_L112R_for	CGAGAAGGTGGAGCGGCAGGAGCTCAATG	SDM
DES_L112R_rev	CATTGAGCTCCTGCCGCTCCACCTTCTCG	SDM
DES_E114G_for	GTGGAGCTGCAGGGGCTCAATGACCGC	SDM
DES_E114G_rev	GCGGTCATTGAGCCCCTGCAGCTCCAC	SDM
DES_L115P_for	GGAGCTGCAGGAGCCCAATGACCGCTTCG	SDM
DES_L115P_rev	CGAAGCGGTCATTGGGCTCCTGCAGCTCC	SDM
DES_N116I_for	GTGGAGCTGCAGGAGCTCATTGACCGCTTC	SDM
DES_N116I_rev	GAAGCGGTCAATGAGCTCCTGCAGCTCCAC	SDM
DES_N116K_for	GGAGCTGCAGGAGCTCAAGGACCGCTTCG	SDM
DES_N116K_rev	CGAAGCGGTCCTTGAGCTCCTGCAGCTCC	SDM
DES_D117H_for	GGAGCTGCAGGAGCTCAATCACCGCTTCGC	SDM
DES_D117H_rev	GCGAAGCGGTGATTGAGCTCCTGCAGCTCC	SDM
DES_R118C_for	GCAGGAGCTCAATGACTGCTTCGCCAACTACAT	SDM
DES_R118C_rev	ATGTAGTTGGCGAAGCAGTCATTGAGCTCCTGC	SDM
DES_R118S_for	GCAGGAGCTCAATGACAGCTTCGCCAACTACAT	SDM
DES_R118S_rev	ATGTAGTTGGCGAAGCTGTCATTGAGCTCCTGC	SDM
DES_A120P_for	GCTCAATGACCGCTTCCCCAACTACATCGAGAA	SDM
DES_A120P_rev	TTCTCGATGTAGTTGGGGAAGCGGTCATTGAGC	SDM
DES_N121H_for	CAATGACCGCTTCGCCCACTACATCGAGAAGGT	SDM
DES_N121H_rev	ACCTTCTCGATGTAGTGGGCGAAGCGGTCATTG	SDM
DES_Y122D_for	GACCGCTTCGCCAACGACATCGAGAAGGTGC	SDM
DES_Y122D_rev	GCACCTTCTCGATGTCGTTGGCGAAGCGG	SDM
DES_Y122C_for	CCGCTTCGCCAACTGCATCGAGAAGGTGC	SDM
DES_Y122C_rev	GCACCTTCTCGATGCAGTTGGCGAAGCGG	SDM
DES_I123V_for	GCTTCGCCAACTACGTCGAGAAGGTGCGC	SDM
DES_I123V_rev	GCGCACCTTCTCGACGTAGTTGGCGAAGC	SDM
DES_I123N_for	ACCGCTTCGCCAACTACAACGAGAAGGTGC	SDM
DES_I123N_rev	GCACCTTCTCGTTGTAGTTGGCGAAGCGGT	SDM
DES_E124G_for	CGCCAACTACATCGGGAAGGTGCGCTTCC	SDM
DES_E124G_rev	GGAAGCGCACCTTCCCGATGTAGTTGGCG	SDM
DES_E124A_for	CGCCAACTACATCGCGAAGGTGCGCTTCC	SDM
DES_E124A_rev	GGAAGCGCACCTTCGCGATGTAGTTGGCG	SDM
DES_V126M_for	CAACTACATCGAGAAGATGCGCTTCCTGGAGCA	SDM

Preprints (www.preprints.org) | NOT PEER-REVIEWED | Posted: 8 August 2022 doi:10.20944/preprints202208.0152.v1

Name	Sequence (5′-3′)	Application
DES_V126M_rev	TGCTCCAGGAAGCGCATCTTCTCGATGTAGTTG	SDM
DES_V126L_for	CAACTACATCGAGAAGTTGCGCTTCCTGGAGCA	SDM
DES_V126L_rev	TGCTCCAGGAAGCGCAACTTCTCGATGTAGTTG	SDM
DES_R127G_for	ACATCGAGAAGGTGGGCTTCCTGGAGCAG	SDM
DES_R127G_rev	CTGCTCCAGGAAGCCCACCTTCTCGATGT	SDM
DES_R127P_for	CATCGAGAAGGTGCCCTTCCTGGAGCAGC	SDM
DES_R127P_rev	GCTGCTCCAGGAAGGGCACCTTCTCGATG	SDM
DES_L129R_for	GAAGGTGCGCTTCCGGGAGCAGCAGAACG	SDM
DES_L129R_rev	CGTTCTGCTGCTCCCGGAAGCGCACCTTC	SDM
DES_Q131K_for	GCGCTTCCTGGAGAAGCAGAACGCGGC	SDM
DES_Q131K_rev	GCCGCGTTCTGCTTCTCCAGGAAGCGC	SDM
DES_A135V_for	GCAGAACGCGGTGCTCGCCGCCG	SDM
DES_A135V_rev	CGGCGGCGAGCACCGCGTTCTGC	SDM
DES_L136V_for	AGAACGCGGCGGTCGCCGCCGAA	SDM
DES_L136V_rev	TTCGGCGGCGACCGCCGCGTTCT	SDM
DES_L136H_for	GAACGCGGCGCACGCCGCCGAAG	SDM
DES_L136H_rev	CTTCGGCGGCGTGCGCCGCGTTC	SDM
DES_A137D_for	CGCGGCGCTCGACGCCGAAGTGA	SDM
DES_A137D_rev	TCACTTCGGCGTCGAGCGCCGCG	SDM
DES_E139Q_for	GCGCTCGCCGCCCAGGTGAACCGGCTC	SDM
DES_E139Q_rev	GAGCCGGTTCACCTGGGCGGCGAGCGC	SDM
DES_E139K_for	GCGCTCGCCGCCAAAGTGAACCGGC	SDM
DES_E139K_rev	GCCGGTTCACTTTGGCGGCGAGCGC	SDM
DES_V140M_for	CGCTCGCCGCCGAAATGAACCGGCTC	SDM
DES_V140M_rev	GAGCCGGTTCATTTCGGCGGCGAGCG	SDM
DES_V140L_for	CGCTCGCCGCCGAATTGAACCGGCTC	SDM
DES_V140L_rev	GAGCCGGTTCAATTCGGCGGCGAGCG	SDM
DES_L143V_for	GAAGTGAACCGGGTCAAGGGCCGCG	SDM
DES_L143V_rev	CGCGGCCCTTGACCCGGTTCACTTC	SDM
DES_L143P_for	GAAGTGAACCGGCCCAAGGGCCGCGAG	SDM
DES_L143P_rev	CTCGCGGCCCTTGGGCCGGTTCACTTC	SDM
DES_G145D_for	CCGGCTCAAGGACCGCGAGCCGA	SDM
DES_G145D_rev	TCGGCTCGCGGTCCTTGAGCCGG	SDM
CMV_for	CGCAAATGGGCGGTAGGCGTG	Sanger sequencing
EGFP_rev	CGTCGCCGTCCAGCTCGACCAG	Sanger sequencing

* SDM = site-directed mutagenesis.

References

1. Brodehl, A.; Gaertner-Rommel, A.; Milting, H. Molecular insights into cardiomyopathies associated with desmin (DES) mutations. *Biophys Rev* **2018**, *10*, 983-1006, doi:10.1007/s12551-018-0429-0.
2. Maggi, L.; Mavroidis, M.; Psarras, S.; Capetanaki, Y.; Lattanzi, G. Skeletal and Cardiac Muscle Disorders Caused by Mutations in Genes Encoding Intermediate Filament Proteins. *Int J Mol Sci* **2021**, *22*, doi:10.3390/ijms22084256.
3. Brodehl, A.; Dieding, M.; Biere, N.; Unger, A.; Klauke, B.; Walhorn, V.; Gummert, J.; Schulz, U.; Linke, W.A.; Gerull, B.; et al. Functional characterization of the novel DES mutation p.L136P associated with dilated cardiomyopathy reveals a dominant filament assembly defect. *J Mol Cell Cardiol* **2016**, *91*, 207-214, doi:10.1016/j.yjmcc.2015.12.015.
4. Huang, Y.S.; Xing, Y.L.; Li, H.W. Heterozygous desmin gene (DES) mutation contributes to familial dilated cardiomyopathy. *J Int Med Res* **2021**, *49*, 3000605211006598, doi:10.1177/03000605211006598.

5. Fischer, B.; Dittmann, S.; Brodehl, A.; Unger, A.; Stallmeyer, B.; Paul, M.; Seebohm, G.; Kayser, A.; Peischard, S.; Linke, W.A.; et al. Functional characterization of novel alpha-helical rod domain desmin (DES) pathogenic variants associated with dilated cardiomyopathy, atrioventricular block and a risk for sudden cardiac death. *Int J Cardiol* **2021**, *329*, 167-174, doi:10.1016/j.ijcard.2020.12.050.
6. Protonotarios, A.; Brodehl, A.; Asimaki, A.; Jager, J.; Quinn, E.; Stanasiuk, C.; Ratnavadivel, S.; Futema, M.; Akhtar, M.M.; Gossios, T.D.; et al. The Novel Desmin Variant p.Leu115Ile Is Associated With a Unique Form of Biventricular Arrhythmogenic Cardiomyopathy. *Can J Cardiol* **2021**, *37*, 857-866, doi:10.1016/j.cjca.2020.11.017.
7. Bermudez-Jimenez, F.J.; Carriel, V.; Brodehl, A.; Alaminos, M.; Campos, A.; Schirmer, I.; Milting, H.; Abril, B.A.; Alvarez, M.; Lopez-Fernandez, S.; et al. Novel Desmin Mutation p.Glu401Asp Impairs Filament Formation, Disrupts Cell Membrane Integrity, and Causes Severe Arrhythmogenic Left Ventricular Cardiomyopathy/Dysplasia. *Circulation* **2018**, *137*, 1595-1610, doi:10.1161/CIRCULATIONAHA.117.028719.
8. Oka, H.; Nakau, K.; Imanishi, R.; Furukawa, T.; Tanabe, Y.; Hirono, K.; Hata, Y.; Nishida, N.; Azuma, H. A Case Report of a Rare Heterozygous Variant in the Desmin Gene Associated With Hypertrophic Cardiomyopathy and Complete Atrioventricular Block. *CJC Open* **2021**, *3*, 1195-1198, doi:10.1016/j.cjco.2021.05.003.
9. Harada, H.; Hayashi, T.; Nishi, H.; Kusaba, K.; Koga, Y.; Koga, Y.; Nonaka, I.; Kimura, A. Phenotypic expression of a novel desmin gene mutation: hypertrophic cardiomyopathy followed by systemic myopathy. *J Hum Genet* **2018**, *63*, 249-254, doi:10.1038/s10038-017-0383-x.
10. Brodehl, A.; Gerull, B. Genetic Insights into Primary Restrictive Cardiomyopathy. *J Clin Med* **2022**, *11*, doi:10.3390/jcm11082094.
11. Brodehl, A.; Hain, C.; Flottmann, F.; Ratnavadivel, S.; Gaertner, A.; Klauke, B.; Kalinowski, J.; Korperich, H.; Gummert, J.; Paluszkiewicz, L.; et al. The Desmin Mutation DES-c.735G>C Causes Severe Restrictive Cardiomyopathy by Inducing In-Frame Skipping of Exon-3. *Biomedicines* **2021**, *9*, doi:10.3390/biomedicines9101400.
12. Kulikova, O.; Brodehl, A.; Kiseleva, A.; Myasnikov, R.; Meshkov, A.; Stanasiuk, C.; Gartner, A.; Divashuk, M.; Sotnikova, E.; Koretskiy, S.; et al. The Desmin (DES) Mutation p.A337P Is Associated with Left-Ventricular Non-Compaction Cardiomyopathy. *Genes (Basel)* **2021**, *12*, doi:10.3390/genes12010121.
13. Marakhonov, A.V.; Brodehl, A.; Myasnikov, R.P.; Sparber, P.A.; Kiseleva, A.V.; Kulikova, O.V.; Meshkov, A.N.; Zharikova, A.A.; Koretsky, S.N.; Kharlap, M.S.; et al. Noncompaction cardiomyopathy is caused by a novel in-frame desmin (DES) deletion mutation within the 1A coiled-coil rod segment leading to a severe filament assembly defect. *Hum Mutat* **2019**, *40*, 734-741, doi:10.1002/humu.23747.
14. Bergman, J.E.; Veenstra-Knol, H.E.; van Essen, A.J.; van Ravenswaaij, C.M.; den Dunnen, W.F.; van den Wijngaard, A.; van Tintelen, J.P. Two related Dutch families with a clinically variable presentation of cardioskeletal myopathy caused by a novel S13F mutation in the desmin gene. *Eur J Med Genet* **2007**, *50*, 355-366, doi:10.1016/j.ejmg.2007.06.003.
15. Goldfarb, L.G.; Park, K.Y.; Cervenakova, L.; Gorokhova, S.; Lee, H.S.; Vasconcelos, O.; Nagle, J.W.; Semino-Mora, C.; Sivakumar, K.; Dalakas, M.C. Missense mutations in desmin associated with familial cardiac and skeletal myopathy. *Nat Genet* **1998**, *19*, 402-403, doi:10.1038/1300.
16. Munoz-Marmol, A.M.; Strasser, G.; Isamat, M.; Coulombe, P.A.; Yang, Y.; Roca, X.; Vela, E.; Mate, J.L.; Coll, J.; Fernandez-Figueras, M.T.; et al. A dysfunctional desmin mutation in a patient with severe generalized myopathy. *Proc Natl Acad Sci U S A* **1998**, *95*, 11312-11317, doi:10.1073/pnas.95.19.11312.
17. Li, Z.L.; Lilienbaum, A.; Butler-Browne, G.; Paulin, D. Human desmin-coding gene: complete nucleotide sequence, characterization and regulation of expression during myogenesis and development. *Gene* **1989**, *78*, 243-254, doi:10.1016/0378-1119(89)90227-8.
18. Cetin, N.; Balci-Hayta, B.; Gundesli, H.; Korkusuz, P.; Purali, N.; Talim, B.; Tan, E.; Selcen, D.; Erdem-Ozdamar, S.; Dincer, P. A novel desmin mutation leading to autosomal recessive limb-girdle muscular dystrophy: distinct histopathological outcomes compared with desminopathies. *J Med Genet* **2013**, *50*, 437-443, doi:10.1136/jmedgenet-2012-101487.

19. McLaughlin, H.M.; Kelly, M.A.; Hawley, P.P.; Darras, B.T.; Funke, B.; Picker, J. Compound heterozygosity of predicted loss-of-function DES variants in a family with recessive desminopathy. *BMC Med Genet* **2013**, *14*, 68, doi:10.1186/1471-2350-14-68.
20. Agnetti, G.; Herrmann, H.; Cohen, S. New roles for desmin in the maintenance of muscle homeostasis. *FEBS J* **2022**, *289*, 2755-2770, doi:10.1111/febs.15864.
21. Granger, B.L.; Lazarides, E. The existence of an insoluble Z disc scaffold in chicken skeletal muscle. *Cell* **1978**, *15*, 1253-1268, doi:10.1016/0092-8674(78)90051-x.
22. Ervasti, J.M. Costameres: the Achilles' heel of Herculean muscle. *J Biol Chem* **2003**, *278*, 13591-13594, doi:10.1074/jbc.R200021200.
23. Choi, H.J.; Park-Snyder, S.; Pascoe, L.T.; Green, K.J.; Weis, W.I. Structures of two intermediate filament-binding fragments of desmoplakin reveal a unique repeat motif structure. *Nat Struct Biol* **2002**, *9*, 612-620, doi:10.1038/nsb818.
24. Lowery, J.; Kuczmarski, E.R.; Herrmann, H.; Goldman, R.D. Intermediate Filaments Play a Pivotal Role in Regulating Cell Architecture and Function. *J Biol Chem* **2015**, *290*, 17145-17153, doi:10.1074/jbc.R115.640359.
25. Goldfarb, L.G.; Dalakas, M.C. Tragedy in a heartbeat: malfunctioning desmin causes skeletal and cardiac muscle disease. *J Clin Invest* **2009**, *119*, 1806-1813, doi:10.1172/JCI38027.
26. Herrmann, H.; Aebi, U. Intermediate Filaments: Structure and Assembly. *Cold Spring Harb Perspect Biol* **2016**, *8*, doi:10.1101/cshperspect.a018242.
27. Vermeire, P.J.; Stalmans, G.; Lilina, A.V.; Fiala, J.; Novak, P.; Herrmann, H.; Strelkov, S.V. Molecular Interactions Driving Intermediate Filament Assembly. *Cells* **2021**, *10*, doi:10.3390/cells10092457.
28. Chernyatina, A.A.; Nicolet, S.; Aebi, U.; Herrmann, H.; Strelkov, S.V. Atomic structure of the vimentin central alpha-helical domain and its implications for intermediate filament assembly. *Proc Natl Acad Sci U S A* **2012**, *109*, 13620-13625, doi:10.1073/pnas.1206836109.
29. Herrmann, H.; Strelkov, S.V.; Feja, B.; Rogers, K.R.; Brettel, M.; Lustig, A.; Haner, M.; Parry, D.A.; Steinert, P.M.; Burkhard, P.; et al. The intermediate filament protein consensus motif of helix 2B: its atomic structure and contribution to assembly. *J Mol Biol* **2000**, *298*, 817-832, doi:10.1006/jmbi.2000.3719.
30. Herrmann, H.; Haner, M.; Brettel, M.; Ku, N.O.; Aebi, U. Characterization of distinct early assembly units of different intermediate filament proteins. *J Mol Biol* **1999**, *286*, 1403-1420, doi:10.1006/jmbi.1999.2528.
31. Winheim, S.; Hieb, A.R.; Silbermann, M.; Surmann, E.M.; Wedig, T.; Herrmann, H.; Langowski, J.; Mucke, N. Deconstructing the late phase of vimentin assembly by total internal reflection fluorescence microscopy (TIRFM). *PLoS One* **2011**, *6*, e19202, doi:10.1371/journal.pone.0019202.
32. Colakoglu, G.; Brown, A. Intermediate filaments exchange subunits along their length and elongate by end-to-end annealing. *J Cell Biol* **2009**, *185*, 769-777, doi:10.1083/jcb.200809166.
33. Bar, H.; Mucke, N.; Kostareva, A.; Sjoberg, G.; Aebi, U.; Herrmann, H. Severe muscle disease-causing desmin mutations interfere with in vitro filament assembly at distinct stages. *Proc Natl Acad Sci U S A* **2005**, *102*, 15099-15104, doi:10.1073/pnas.0504568102.
34. Brodehl, A.; Hedde, P.N.; Dieding, M.; Fatima, A.; Walhorn, V.; Gayda, S.; Saric, T.; Klauke, B.; Gummert, J.; Anselmetti, D.; et al. Dual color photoactivation localization microscopy of cardiomyopathy-associated desmin mutants. *J Biol Chem* **2012**, *287*, 16047-16057, doi:10.1074/jbc.M111.313841.
35. Richards, S.; Aziz, N.; Bale, S.; Bick, D.; Das, S.; Gastier-Foster, J.; Grody, W.W.; Hegde, M.; Lyon, E.; Spector, E.; et al. Standards and guidelines for the interpretation of sequence variants: a joint consensus recommendation of the American College of Medical Genetics and Genomics and the Association for Molecular Pathology. *Genet Med* **2015**, *17*, 405-424, doi:10.1038/gim.2015.30.

36. Klauke, B.; Kossmann, S.; Gaertner, A.; Brand, K.; Stork, I.; Brodehl, A.; Dieding, M.; Walhorn, V.; Anselmetti, D.; Gerdes, D.; et al. De novo desmin-mutation N116S is associated with arrhythmogenic right ventricular cardiomyopathy. *Hum Mol Genet* **2010**, *19*, 4595-4607, doi:10.1093/hmg/ddq387.
37. Brodehl, A.; Pour Hakimi, S.A.; Stanasiuk, C.; Ratnavadivel, S.; Hendig, D.; Gaertner, A.; Gerull, B.; Gummert, J.; Paluszkiewicz, L.; Milting, H. Restrictive Cardiomyopathy is Caused by a Novel Homozygous Desmin (DES) Mutation p.Y122H Leading to a Severe Filament Assembly Defect. *Genes (Basel)* **2019**, *10*, doi:10.3390/genes10110918.
38. Brodehl, A.; Dieding, M.; Klauke, B.; Dec, E.; Madaan, S.; Huang, T.; Gargus, J.; Fatima, A.; Saric, T.; Cakar, H.; et al. The novel desmin mutant p.A120D impairs filament formation, prevents intercalated disk localization, and causes sudden cardiac death. *Circ Cardiovasc Genet* **2013**, *6*, 615-623, doi:10.1161/CIRCGENETICS.113.000103.
39. Vernengo, L.; Chourbagi, O.; Panuncio, A.; Lilienbaum, A.; Batonnet-Pichon, S.; Bruston, F.; Rodrigues-Lima, F.; Mesa, R.; Pizzarossa, C.; Demay, L.; et al. Desmin myopathy with severe cardiomyopathy in a Uruguayan family due to a codon deletion in a new location within the desmin 1A rod domain. *Neuromuscul Disord* **2010**, *20*, 178-187, doi:10.1016/j.nmd.2010.01.001.
40. Landrum, M.J.; Chitipiralla, S.; Brown, G.R.; Chen, C.; Gu, B.; Hart, J.; Hoffman, D.; Jang, W.; Kaur, K.; Liu, C.; et al. ClinVar: improvements to accessing data. *Nucleic Acids Res* **2020**, *48*, D835-D844, doi:10.1093/nar/gkz972.
41. Stenson, P.D.; Mort, M.; Ball, E.V.; Evans, K.; Hayden, M.; Heywood, S.; Hussain, M.; Phillips, A.D.; Cooper, D.N. The Human Gene Mutation Database: towards a comprehensive repository of inherited mutation data for medical research, genetic diagnosis and next-generation sequencing studies. *Hum Genet* **2017**, *136*, 665-677, doi:10.1007/s00439-017-1779-6.
42. Hedberg, K.K.; Chen, L.B. Absence of intermediate filaments in a human adrenal cortex carcinoma-derived cell line. *Exp Cell Res* **1986**, *163*, 509-517, doi:10.1016/0014-4827(86)90081-9.
43. Hescheler, J.; Meyer, R.; Plant, S.; Krautwurst, D.; Rosenthal, W.; Schultz, G. Morphological, biochemical, and electrophysiological characterization of a clonal cell (H9c2) line from rat heart. *Circ Res* **1991**, *69*, 1476-1486, doi:10.1161/01.res.69.6.1476.
44. Evans, R.; O'Neill, M.; Pritzel, A.; Antropova, N.; Senior, A.; Green, T.; Žídek, A.; Bates, R.; Blackwell, S.; Yim, J.; et al. Protein complex prediction with AlphaFold-Multimer. **2022**, 2021.2010.2004.463034, doi:10.1101/2021.10.04.463034 %J bioRxiv.
45. Hsu, L.A.; Ko, Y.S.; Yeh, Y.H.; Chang, C.J.; Chan, Y.H.; Kuo, C.T.; Tsai, H.Y.; Chang, G.J. A Novel DES L115F Mutation Identified by Whole Exome Sequencing is Associated with Inherited Cardiac Conduction Disease. *Int J Mol Sci* **2019**, *20*, doi:10.3390/ijms20246227.
46. Bar, H.; Goudeau, B.; Walde, S.; Casteras-Simon, M.; Mucke, N.; Shatunov, A.; Goldberg, Y.P.; Clarke, C.; Holton, J.L.; Eymard, B.; et al. Conspicuous involvement of desmin tail mutations in diverse cardiac and skeletal myopathies. *Hum Mutat* **2007**, *28*, 374-386, doi:10.1002/humu.20459.
47. Bar, H.; Kostareva, A.; Sjoberg, G.; Sejersen, T.; Katus, H.A.; Herrmann, H. Forced expression of desmin and desmin mutants in cultured cells: impact of myopathic missense mutations in the central coiled-coil domain on network formation. *Exp Cell Res* **2006**, *312*, 1554-1565, doi:10.1016/j.yexcr.2006.01.021.
48. Kreplak, L.; Bar, H. Severe myopathy mutations modify the nanomechanics of desmin intermediate filaments. *J Mol Biol* **2009**, *385*, 1043-1051, doi:10.1016/j.jmb.2008.10.095.
49. Prust, M.; Wang, J.; Morizono, H.; Messing, A.; Brenner, M.; Gordon, E.; Hartka, T.; Sokohl, A.; Schiffmann, R.; Gordish-Dressman, H.; et al. GFAP mutations, age at onset, and clinical subtypes in Alexander disease. *Neurology* **2011**, *77*, 1287-1294, doi:10.1212/WNL.0b013e3182309f72.
50. Li, R.; Johnson, A.B.; Salomons, G.; Goldman, J.E.; Naidu, S.; Quinlan, R.; Cree, B.; Ruyle, S.Z.; Banwell, B.; D'Hooghe, M.; et al. Glial fibrillary acidic protein mutations in infantile, juvenile, and adult forms of Alexander disease. *Ann Neurol* **2005**, *57*, 310-326, doi:10.1002/ana.20406.
51. Brenner, M.; Johnson, A.B.; Boespflug-Tanguy, O.; Rodriguez, D.; Goldman, J.E.; Messing, A. Mutations in GFAP, encoding glial fibrillary acidic protein, are associated with Alexander disease. *Nat Genet* **2001**, *27*, 117-120, doi:10.1038/83679.

 doi:10.20944/preprints202208.0152.v1

52. Gorospe, J.R.; Naidu, S.; Johnson, A.B.; Puri, V.; Raymond, G.V.; Jenkins, S.D.; Pedersen, R.C.; Lewis, D.; Knowles, P.; Fernandez, R.; et al. Molecular findings in symptomatic and pre-symptomatic Alexander disease patients. *Neurology* **2002**, *58*, 1494-1500, doi:10.1212/wnl.58.10.1494.

53. Tan, D.; Yang, H.; Yuan, Y.; Bonnemann, C.; Chang, X.; Wang, S.; Wu, Y.; Wu, X.; Xiong, H. Phenotype-Genotype Analysis of Chinese Patients with Early-Onset LMNA-Related Muscular Dystrophy. *PLoS One* **2015**, *10*, e0129699, doi:10.1371/journal.pone.0129699.

54. Benedetti, S.; Menditto, I.; Degano, M.; Rodolico, C.; Merlini, L.; D'Amico, A.; Palmucci, L.; Berardinelli, A.; Pegoraro, E.; Trevisan, C.P.; et al. Phenotypic clustering of lamin A/C mutations in neuromuscular patients. *Neurology* **2007**, *69*, 1285-1292, doi:10.1212/01.wnl.0000261254.87181.80.

55. Prigogine, C.; Richard, P.; Van den Bergh, P.; Groswasser, J.; Deconinck, N. Novel LMNA mutation presenting as severe congenital muscular dystrophy. *Pediatr Neurol* **2010**, *43*, 283-286, doi:10.1016/j.pediatrneurol.2010.05.016.